Modelling Floods with Graph Neural Networks

Roberto Bentivoglio, Elvin Isufi, Sebastiaan Jonkman, Riccardo Taormina

Date: 03/04/25

TU Delft

AIAI ADRO ILAB

Why do we care about flood modelling?

→ Flood risk

→ Early warning systems

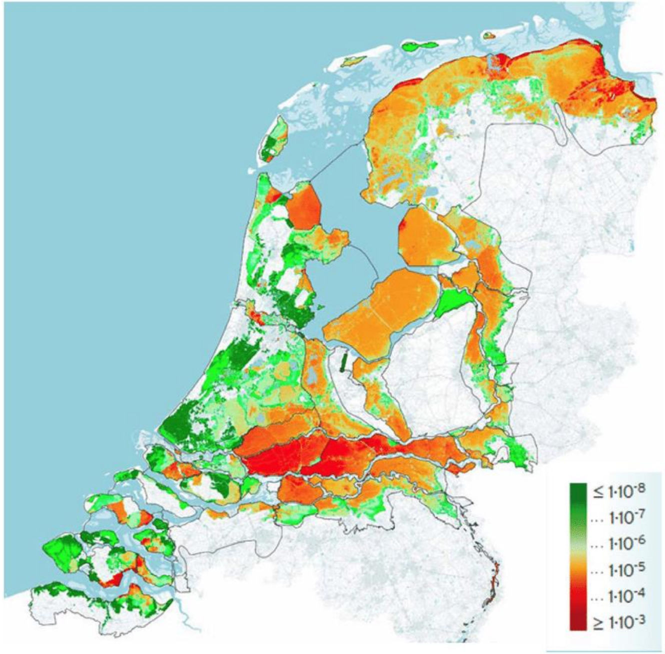

Sebastiaan N. Jonkman, Hessel G. Voortman, Wouter Jan Klerk & Saskia van Vuren (2018) Developments in the management of flood defences and hydraulic infrastructure in the Netherlands, Structure and Infrastructure Engineering, 14:7, 895-910,
DOI: 10.1080/15732479.2018.1441317

Motivation

- Accurate numerical models are computationally expensive
- Deep learning methods can be used to accelerate simulations
- Current models cannot predict the spatio-temporal evolution of floods for unseen topographies

TU Delft

AI AI
ADRO
ILAB

SWE-GNN

Overview

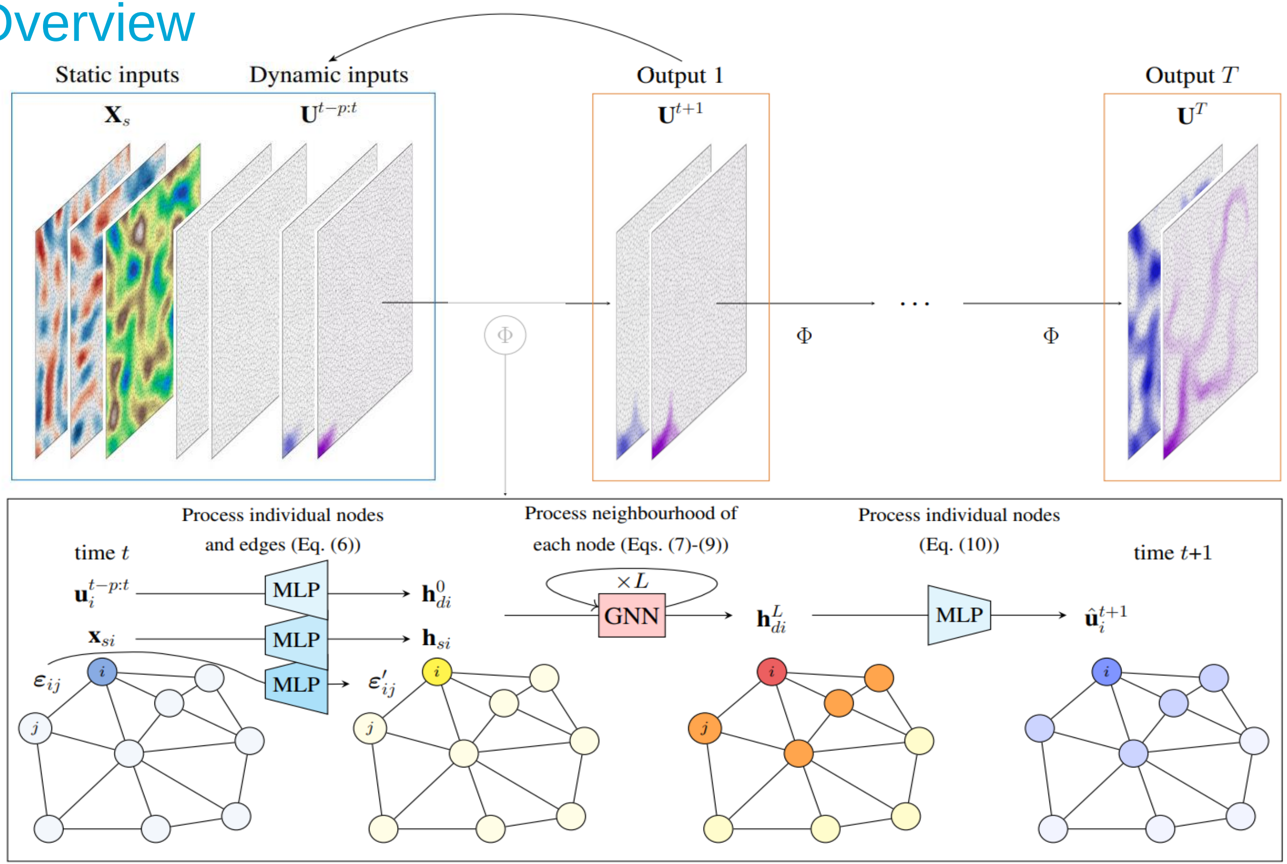

SWE-GNN

Motivation

$$\boldsymbol{u}_i^{t+1} = \boldsymbol{u}_i^t + \sum_{j=1}^{N_i}\left(\boldsymbol{s}_{ij} - (\boldsymbol{F}\cdot\boldsymbol{n})_{ij}\frac{l_{ij}}{\mathrm{a}_i}\right)\Delta t \quad \longleftrightarrow \quad \boldsymbol{x}_i^{t+1} = \boldsymbol{x}_i^t + \sum_{j=1}^{N_i} f(\boldsymbol{x}_i, \boldsymbol{x}_j, \boldsymbol{\varepsilon}_{ij})$$

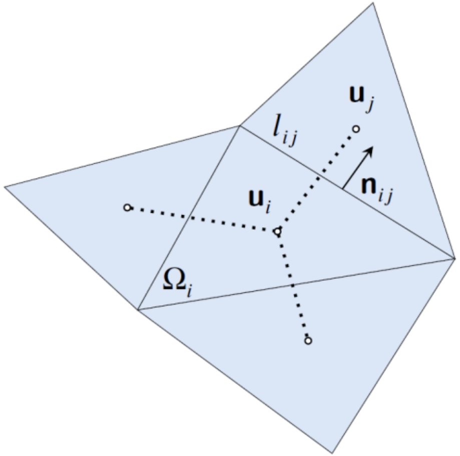

Finite volume mesh

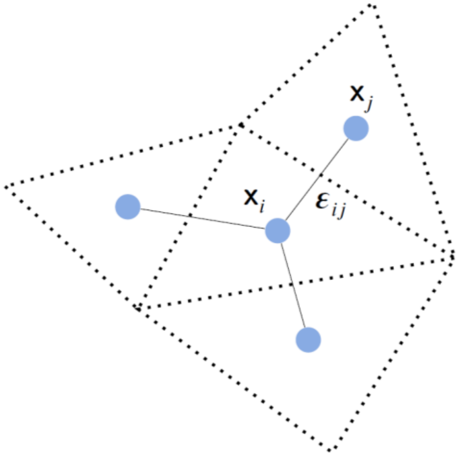

Dual graph

Multi-scale SWE-GNN

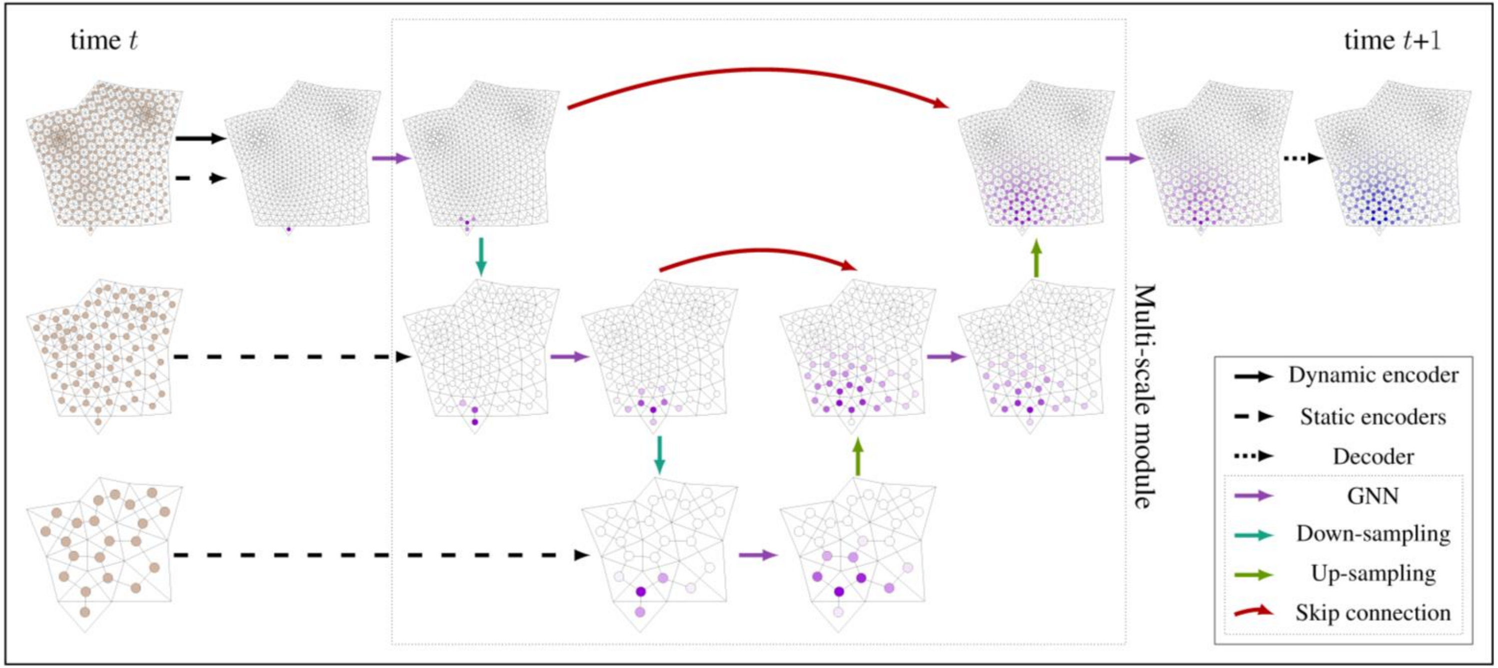

- Idea: each scale propagates water at different speeds

Training strategy

- Multi-step-ahead loss function

$$\mathcal{L} = \frac{1}{HO} \sum_{\tau=1}^{H} \sum_{o=1}^{O} \gamma_o \| \hat{\mathbf{u}}_o^{t+\tau} - \mathbf{u}_o^{t+\tau} \|_2$$

- Curriculum learning
  - Progressively increase prediction horizon H after a fixed amount of training epochs

Training strategy

Curriculum learning

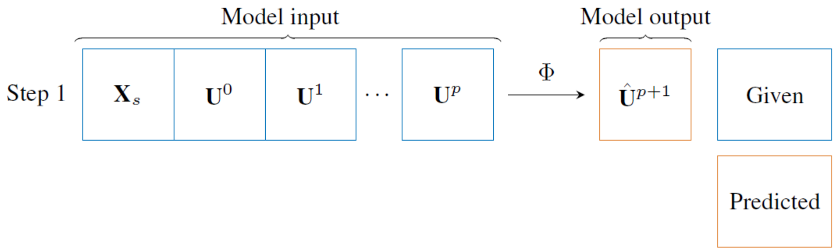

$$\mathcal{L} = \frac{1}{HO} \sum_{\tau=1}^{H} \sum_{o=1}^{O} \gamma_o \|\hat{\mathbf{u}}_o^{t+\tau} - \mathbf{u}_o^{t+\tau}\|_2$$

Dataset

- 60 training, 20 validation, 20 testing simulations
- Varying boundary conditions (peak ranges from 150 to 300 m^3/s)
- Random terrains, random breach location
- 96 hours simulation time, 2h temporal resolution

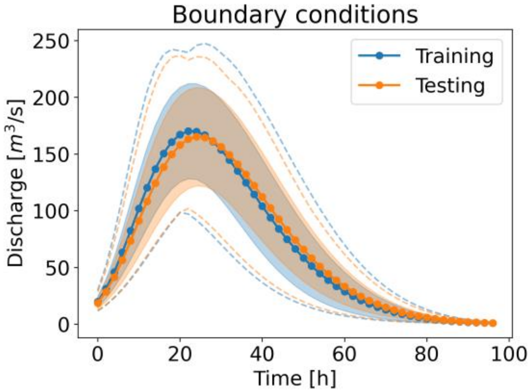

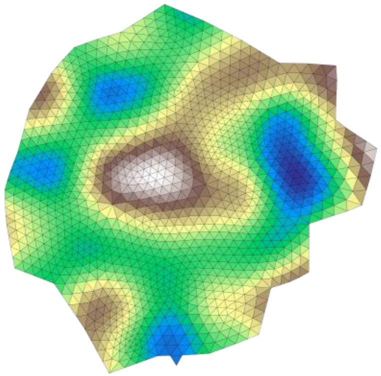

Results

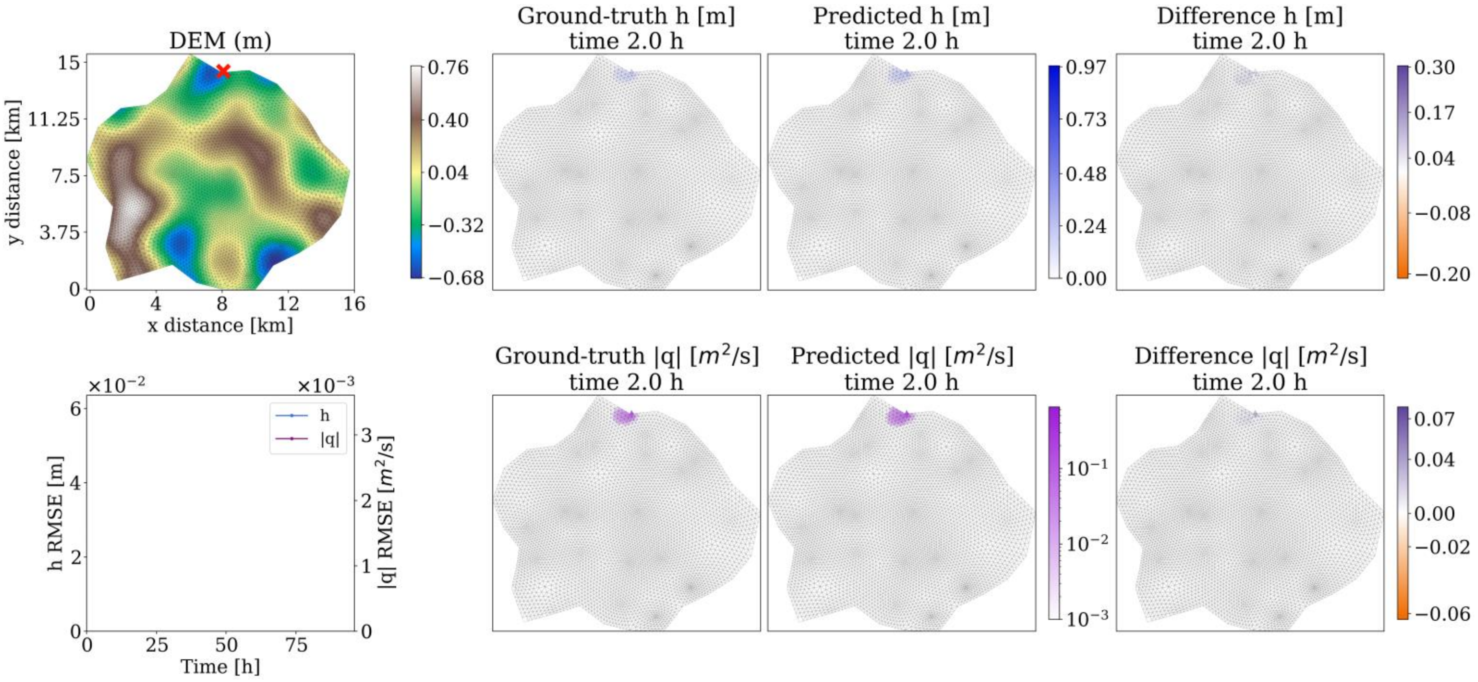

DEM (m)
y distance [km]
x distance [km]
15
11.25
7.5
3.75
0
0
4
8
12
16
0.76
0.40
0.04
−0.32
−0.68
Ground-truth h [m]
time 2.0 h
Predicted h [m]
time 2.0 h
0.97
0.73
0.48
0.24
0.00
Difference h [m]
time 2.0 h
0.30
0.17
0.04
−0.08
−0.20
×10⁻²
×10⁻³
h
|q|
h RMSE [m]
|q| RMSE [m²/s]
Time [h]
6
4
2
0
25
50
75
3
1
Ground-truth |q| [m²/s]
time 2.0 h
Predicted |q| [m²/s]
time 2.0 h
10⁻¹
10⁻²
10⁻³
Difference |q| [m²/s]
time 2.0 h
0.07
0.04
0.00
−0.02
−0.06

Dataset

Case study

- Dike ring 15 Lopiker en Krimpenerwaard in the Netherlands

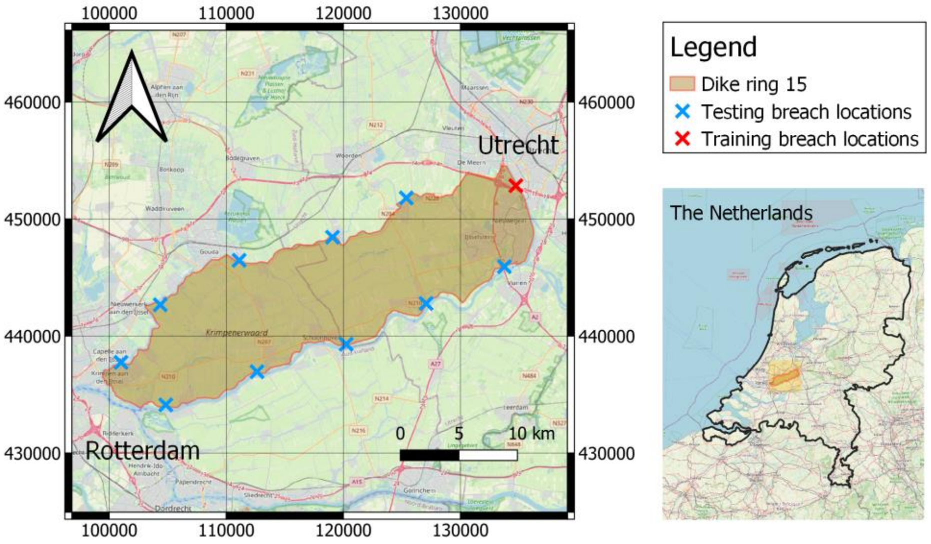

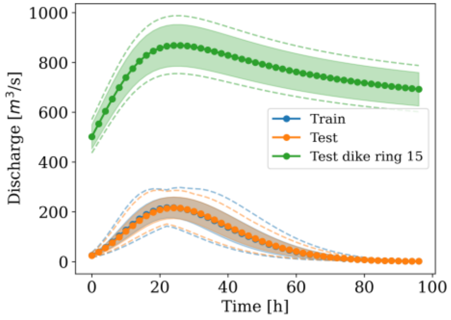

Results

Case study

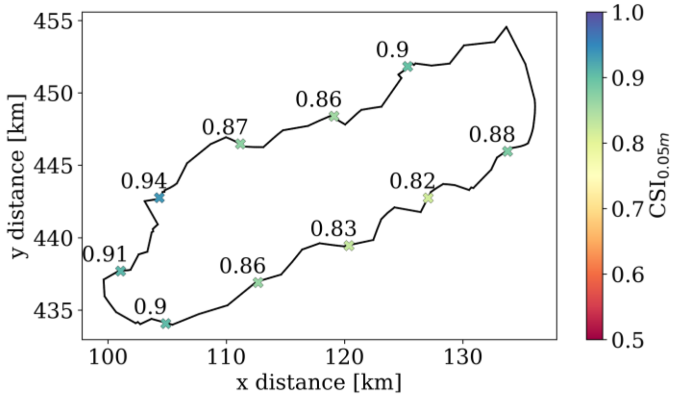

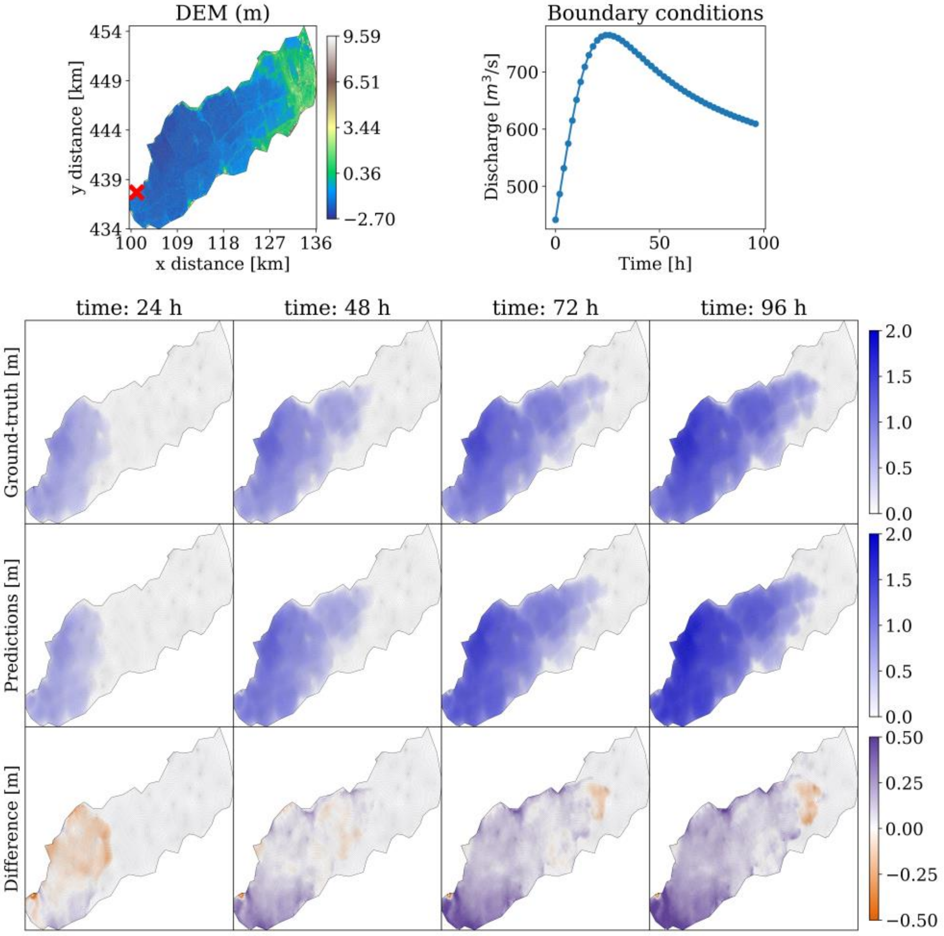

Results

Table 1. Mean and standard deviation of elevation (above sea level), number of cells, cell area, edge length, and total flood volume for the training, validation, and testing datasets. All geometric variables refer to the properties of the finest mesh in each dataset.

Dataset	No. of simulations	Elevation [m]	Number of cells	Cell area [m^2]	Edge length [m]	Flood volume [10^6 m^3]
Train	60	-0.04 ± 0.6	$10\,018 \pm 1251$	$14\,817 \pm 5717$	182.8 ± 37.2	3.07 ± 0.66
Validation	20	-0.06 ± 0.58	$10\,029 \pm 904$	$13\,741 \pm 5125$	176.3 ± 34.9	2.9 ± 0.69
Test	20	-0.03 ± 0.53	9803 ± 1130	$13\,480 \pm 4917$	174.9 ± 33.7	3.02 ± 0.64
Test dike ring 15	10	-1.07 ± 1.17	22 881	$13\,544 \pm 5521$	174.7 ± 36.9	26.5 ± 2.54

Table 2. Effect of fine-tuning the mSWE-GNN model on dike ring 15. The provided uncertainty estimates account for the variability across different simulations. All metrics refer only to the finest mesh.

Fine-tuning	MAE ↓		CSI_τ [%] ↑	
	h [10^{-2} m]	$\lvert q \rvert$ [10^{-2} $m^2\,s^{-1}$]	$\tau = 0.05$ m	$\tau = 0.3$ m
No	31.09 ± 5.42	3.37 ± 1.24	63.36 ± 19.54	46.06 ± 18.62
Yes	12.07 ± 4.19	2.08 ± 0.82	87.68 ± 10.3	81.82 ± 16.07

Results

Table 3. Ablation study on the removal or addition of individual architectural and training components for the synthetic testing dataset. These are using a learnable pooling for the downsampling operator, removing skip connections in Eq. (7), removing the 1D CNN in Eq. (8), and using rotation-dependent inputs. The best results are reported in bold; w/o denotes "without".

DL model		MAE ↓		CSI_τ [%] ↑	
		h [10^{-2} m]	$\lvert q \rvert$ [10^{-2} m^2 s^{-1}]	$\tau = 0.05$ m	$\tau = 0.3$ m
	SWE-GNN	9.52 ± 5.03	0.42 ± 0.16	68.7 ± 18.9	51.7 ± 22.1
	mSWE-GNN	$\mathbf{4.84 \pm 2.3}$	$\mathbf{0.27 \pm 0.13}$	$\mathbf{84.02 \pm 9.18}$	$\mathbf{69.56 \pm 17.25}$
mSWE-GNN	with learnable pooling	5.72 ± 3.09	0.32 ± 0.13	81.23 ± 12.23	63.67 ± 19.66
mSWE-GNN	w/o skip connections	5.22 ± 2.22	0.32 ± 0.15	82.44 ± 10.82	66.81 ± 17.31
mSWE-GNN	w/o 1D CNN	5.57 ± 2.5	0.32 ± 0.14	80.75 ± 10.83	65.03 ± 19.21
mSWE-GNN	w/o rotation-invariant inputs	6.07 ± 2.27	0.34 ± 0.15	79.93 ± 10.18	62.89 ± 18.28

Results

Comparison with SWE-GNN

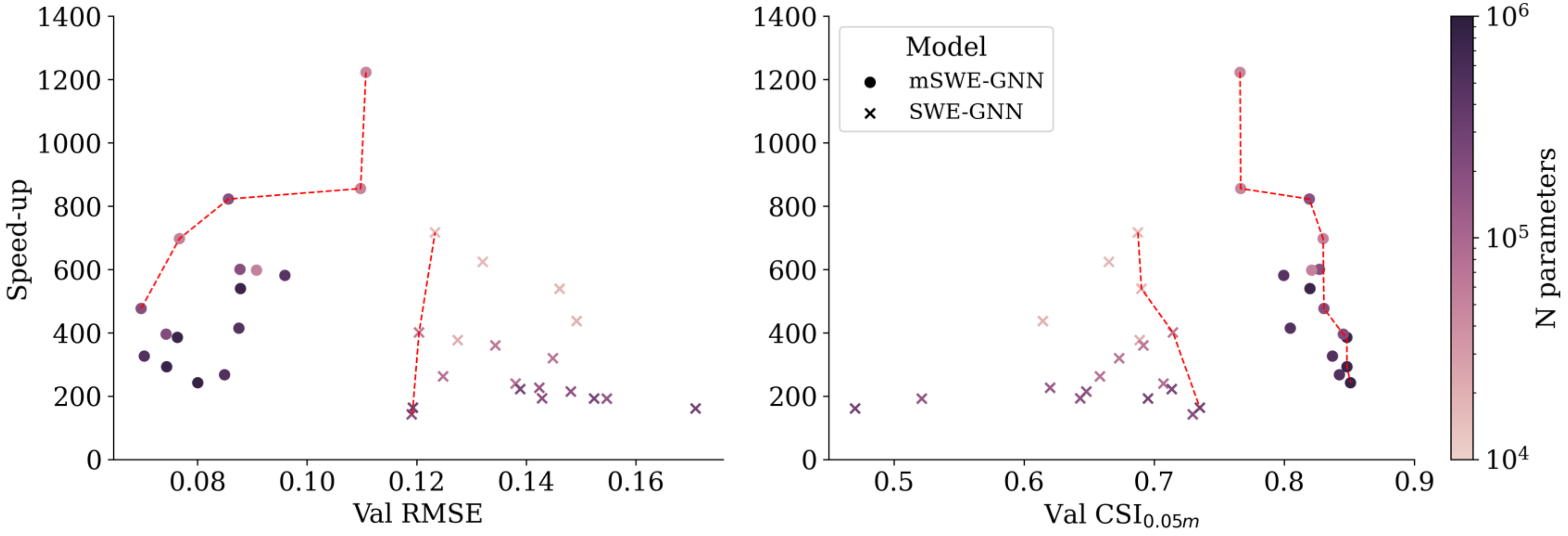

TU Delft AI ADRO ILAB

Conclusions

- We propose a new graph neural network model inspired by finite volume methods for flood modelling

- The proposed model can predict the spatio-temporal evolution of dike-breach floods over
  - unseen topographies,
  - unseen breach locations,
  - unseen boundary conditions,
  - unseen meshes,
  - with speedups up to two orders of magnitude faster

- Future works should aim to apply the model for probabilistic analyses on real case studies